MEASUREMENT OF DIFFERENTIAL CROSS SECTION FOR PROTON-INDUCED DEUTERON BREAKUP AT 108 MeV*

A. Łobejko, B. Jamróz, B. Kłos, E. Stephan, A. Wilczek

Institute of Physics, University of Silesia, 41-500 Chorzów, Poland

A. Kozela, J. Kuboś, P. Kulessa, A. Liptak, W. Parol, B. Włoch

H. Niewodniczański Institute of Nuclear Physics PAN, 31-342 Kraków, Poland

M.T. Bayat, N. Kalantar-Nayestanaki, J. Messchendorp
M. Mohammadi-Dadkan, R. Ramazani-Sharifabadi
H. Tavakoli-Zaniani

KVI-CART, University of Groningen, 9747 AA, Groningen, The Netherlands

G. Khatri, St. Kistryn, J. Zejma

M. Smoluchowski Institute of Physics, Jagiellonian University
30-348 Kraków, Poland

I. Skwira-Chalot

Faculty of Physics, University of Warsaw, 02-093 Warszawa, Poland

(Received December 19, 2018)

The experiment was performed at CCB IFJ PAN in Kraków with the use of the BINA detector. The experimental program and data analysis of proton-induced deuteron breakup reaction at 108 MeV are presented.

DOI:10.5506/APhysPolB.50.361

1. Introduction

Study of features of two nucleon (2N) system dynamics is the basic way to understand the properties of nuclear interactions. The dynamics of the three

* Presented at the Zakopane Conference on Nuclear Physics "Extremes of the Nuclear Landscape", Zakopane, Poland, August 26–September 2, 2018.

nucleons system (3N) is dominated by the contribution from the nucleon–nucleon (NN) interaction, but the theoretical consideration and experimental data show importance of another dynamical ingredient called three-body force (3NF). The role of 3NF in 3N system dynamics can be comprehensively studied by means of the nucleon–deuteron breakup reaction [1–3].

To compare accurate theoretical calculations with the experimental data, a series of experiments was carried out at KVI Groningen and FZ-Jülich to determine cross section and polarization observables of the $^1\mathrm{H}(d,pp)n$ and $^2\mathrm{H}(p,pp)n$ breakup reactions at intermediate energies [4–10]. As a continuation of these studies, the BINA (Big Instrument for Nuclear-polarization Analysis) detector setup has been installed at the Cyclotron Center Bronowice (CCB) in the Institute of Nuclear Physics, Polish Academy of Sciences (IFJ PAN), Kraków. The range of proton beam energies and features of the detection system constitute the basis for experimental studies of various aspects of the dynamics in three nucleon system as 3NF, Coulomb interaction and relativistic effects at regions of their maximum visibility.

2. Detection system and experimental program

The proton beam was delivered by the isochronous cyclotron Proteus C-235 at the kinetic energy of 108, 135 and 160 MeV and focused on a liquid deuterium target. The reaction products were measured using the BINA detection system which is designed to study the elastic and breakup reactions at intermediate energies. The BINA setup allows to register coincidences of two-charged particles in nearly 4π solid angle, making it possible to study almost full phase-space of few-body scattering reactions. The detector is composed of two main parts, the forward Wall and the backward Ball [11].

The forward Wall consists of a three-plane Multi-Wire Proportional Chamber (MWPC) and an array of almost square in shape ΔE–E telescopes formed by two layers of scintillators. The first layer consists of vertically-placed thin transmission ΔE strips and a second one of horizontally-placed thick stopping E bars. The Wall covers a polar angle (θ) in the range of 10°–32° with full azimuthal angle (ϕ) coverage, and up to $\theta = 37°$ with partial azimuthal angle coverage (due to corners of square-shape active region of the MWPC). The detected charged particles pass first through the MWPC what allows precise reconstruction of their emission angles. In the following, their energies are measured in the ΔE–E detector where they are also identified.

The backward Ball surrounds the target forming a scattering chamber. It is composed out of 149 "phoswitch"-type scintillation detectors and covers the central and backward detection angles (35°–160° in the LAB-reference frame).

3. Data analysis

The first data have been collected for *pd* elastic scattering and the ^{2}H$(p, pp)n$ breakup reaction at three proton beam energies: 108, 135 and 160 MeV. The data analysis presented here is focused on the proton–proton coincidences from the breakup reaction at 108 MeV proton beam energy registered in the forward Wall.

For the energy calibration of E detectors, special runs were performed. Proton beams at energies of 70, 83, 97, 108 and 120 MeV have been scattered at the Al target. The data are compared to Geant4 simulations. Particles registered in dedicated measurements are sorted by the hemisphere (s = right/left) with respect to the beam direction, the E detector number ($N = 0, 1, \ldots, 9$) and polar angle θ. The signals c_1 and c_2 are registered by photomultiplier tubes on both ends of each E detector and combined in the geometrical average $C = \sqrt{c_1\, c_2}$ in order to suppress effects of light attenuation along the bar. The mean energies and the distributions widths are derived from the Gaussian fit applied to the distribution of elastically scattered protons for each combination of s, N, θ. Example of calibration curve is presented in Fig. 1. It shows dependence between measured energies of elastically scattered protons expressed in ADC channels (horizontal axis) and simulated values of relevant energies simulated with the use of Geant4 (vertical one). The calibration curve becomes linear above approximately 50 MeV. Below this value, where the light quenching effect is important due to large stopping power, departure from linearity is expected. Therefore, the calibration curve is described by the equation: $y = aC + \sqrt{b}$, where a, b denote fit parameters.

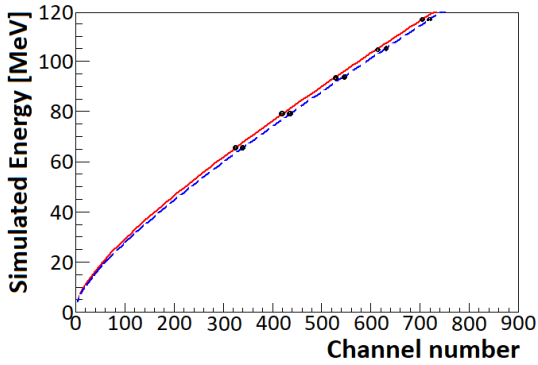

Fig. 1. Example of calibration curves obtained for right side (solid line) and left side (dashed line) of the detector $N = 3$ for a proton emission angle $\theta = 16^\circ \pm 1^\circ$. The statistical uncertainties are smaller than the size of the points. The curves show the relation between ADC conversion unit and the energy deposited in the E detector.

The dependence of the average energy loss of protons on their hit position have been obtained by similar simulation for the proton energies between 15 and 100 MeV and for selected θ angles.

Selection of proton pairs coming from the breakup process and proton–deuteron pairs from the elastic scattering is based on ΔE–E technique of particle identification (PID). As it is shown in Fig. 2 (a), proton and deuteron distributions can be well-distinguished on a ΔE–E scatter plot. Thus, simple graphical cuts are sufficient in order to separate them.

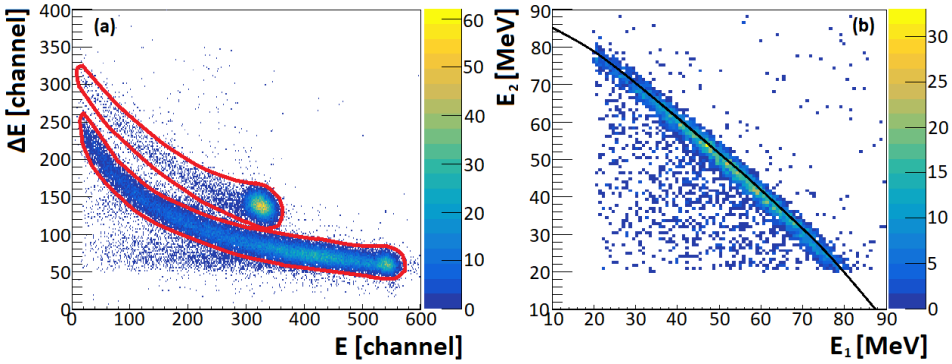

Fig. 2. (a) Example of particle identification spectrum obtained for one combination of thin ΔE and thick E scintillators for beam energy of 108 MeV; good separation of protons (lower band and spot) and deuterons (upper spot) is visible. (b) Kinematical spectrum (correlation of proton energies) obtained for breakup events collected at beam energy of 108 MeV for one selected angular configuration of two protons $\theta_1 = 28°$, $\theta_2 = 30°$, $\phi_{12} = 180°$. The theoretical kinematics line is superimposed.

With proper calibration and efficient selection of the proton–proton coincidences, any kinematic configuration of the breakup reaction (within the angular acceptance of the detection system) can be analyzed. The breakup reaction kinematics is determined by protons momenta $\vec{p_1}$, $\vec{p_2}$. The geometrical configuration is defined by polar angles θ_1, θ_2 of outgoing protons and their relative azimuthal angle ϕ_{12}. The example of kinematical spectrum for one chosen configuration is shown in Fig. 2 (b). The theoretical kinematics line is superimposed on the experimental band. Such a spectrum can be transformed into two other kinematical variables. First one, D, denotes the distance of the point from kinematical curve in the E_1–E_2 plane. Second variable is called S. It is a measure of the arclength along the kinematics. The starting point $S = 0$ is chosen arbitrarily at the place where energy of the second proton reaches minimum. The E_2 *vs.* E_1 plot (Fig. 2 (b)) transformed into S *vs.* D dependence is shown in Fig. 3 (a).

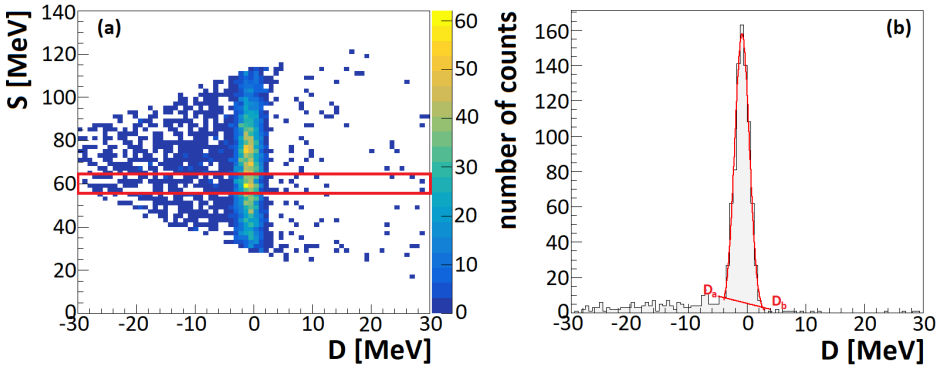

Fig. 3. (a) Transformation of E_2 *vs.* E_1 spectrum presented in the right panel of Fig. 2, to S (arclength) *vs.* D (distance from kinematics) plane. The marked rectangle at $S = 60$ MeV represents a single slice used for background determination. (b) Determination of the background contribution in the slice shown as a rectangle in (a). The background is approximated by a linear function between limits of integration (D_a, D_b).

In order to subtract the background from the S distribution, the S *vs.* D distribution is cut into slices as shown in Fig. 3 (a). Each slice on the S *vs.* D spectrum is treated separately. The background is estimated by a linear function between limits of integration (D_a, D_b) corresponding to distance of $\pm 3\sigma$ from the peak position (*cf.* Fig. 3 (b)). Events below the linear function are subtracted. In Fig. 4, the number of events obtained

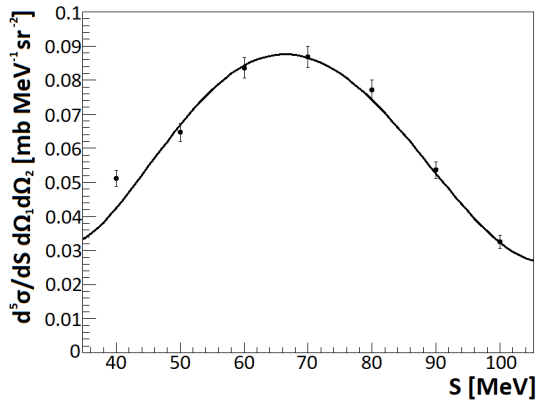

Fig. 4. An example of S distribution of the rate of breakup events obtained for the chosen kinematical configuration: $\theta_1 = 28° \pm 1°$, $\theta_2 = 30° \pm 1°$, $\phi_{12} = 180° \pm 10°$ at 108 MeV beam energy. The experimental data points are compared to theoretical calculation performed by Deltuva *et al.* [12] $CDB + C + \Delta$; normalization of data points is arbitrary.

after the background subtraction is presented as a function of the S for selected kinematical conditions. Arbitrary normalized data are compared to theoretical calculation by Deltuva *et al.* [12] based on the CD-Bonn potential where the 3NF and Coulomb interaction ($CDB+C+\Delta$) have been included. Comparison shows very good agreement of the shape of the experimental S distribution with the theoretical calculations.

4. Outlook

The preliminary analysis of the data taken with the BINA detection setup indicates a proper functioning of the forward part of this detector. In the next steps of data analysis, the determination of detection efficiency and normalization to cross section of elastic scattering are planned. In order to reach the statistical accuracy relevant for studies of the 3NF effects, the next experimental runs with BINA@CCB are foreseen.

This work was partially supported by the National Science Centre, Poland (NCN) from grants UMO-2012/05/B/ST2/02556 and UMO-2016/23/D/ST2/01703.

REFERENCES

[1] St. Kistryn, E. Stephan, *J. Phys. G: Nucl. Part. Phys.* **40**, 063101 (2013).
[2] K. Sagara, *Few-Body Syst.* **48**, 59 (2010).
[3] N. Kalantar-Nayestanaki, E. Epelbaum, J.G. Meschendorp, A. Nogga, *Rep. Prog. Phys.* **75**, 016301 (2012).
[4] St. Kistryn *et al.*, *Phys. Rev. C* **68**, 054004 (2003).
[5] St. Kistryn *et al.*, *Phys. Rev. C* **72**, 044006 (2005).
[6] I. Ciepał *et al.*, *Few-Body Syst.* **56**, 665 (2015).
[7] M. Esami-Kalantari *et al.*, *Mod. Phys. Lett. A* **24**, 839 (2009).
[8] H. Mardanpour *et al.*, *Phys. Lett. B* **687**, 149 (2010).
[9] E. Stephan *et al.*, *Phys. Rev. C* **82**, 014003 (2010).
[10] I. Ciepał *et al.*, *Phys. Rev. C* **85**, 017001 (2012).
[11] A. Rusnok *et al.*, *Acta Phys. Pol. B* **49**, 463 (2018).
[12] A. Deltuva, A.C. Fonseca, P.U. Sauer, *Phys. Rev. C* **72**, 054004 (2005).